Proceedings of the 16th International Conference on Soil Mechanics and Geotechnical Engineering

doi:10.3233/978-1-61499-656-9-913

3D numerical modeling of a geosynthetic-reinforced pile-supported embankment – stress and displacement analysis

Modélisation numérique en 3D du comportement d'un remblai posé sur des pieux renforcés par géosynthétique - analyse d'effort et de déplacement

Jie Huang
Civil, Environmental, & Architectural Engineering (CEAE) Department, the University of Kansas, 2150 Learned Hall, 1530 W. 15th Street, Lawrence, KS 66045, jhuang@ku.edu
James G. Collin
The Collin Group, Ltd. 7445 Arlington Road, Bethesda, MD 20814, USA, jim@thecollingroup.com
Jie Han
Civil, Environmental, & Architectural Engineering (CEAE) Department, the University of Kansas, 2150 Learned Hall, 1530 W. 15th Street, Lawrence, KS 66045, jiehan@ku.edu

ABSTRACT

Piles or columns have been successfully used in combination with geosynthetics to support embankments over soft soil for several decades. The inclusion of geosynthetic reinforcement over piles is to enhance the load transfer from the embankment soil to the piles, reduce total and differential settlements, and increase slope stability. A constructed geosynthetic-reinforced pile-supported embankment to support railways over deep deposits of peat and soft organic soils in Berlin, Germany was selected for numerical modeling and analysis. Precast piles and caps and a load transfer platform consisting of three layers of geogrid reinforcement and granular materials were utilized in this project. A finite difference method, incorporated in the FLAC 3D software, was employed to model this embankment. In the numerical analysis, piles were modeled using pile elements and caps were model as an elastic material. Geogrid elements built in the software were used for representing the geogrid reinforcement. Embankment fill, soft soil, firm soil, and platform fill material were modeled as linearly elastic perfectly plastic materials with Mohr-Coulomb failure criteria. The effects of variations of soft soil modulus below the embankment on the vertical displacements, stresses above pile caps, bending moments on the piles, and tension in reinforcements were investigated. The computed settlements of the embankment and the tension in reinforcements were compared against the measured results.

RÉSUMÉ

Des pieux ou colonnes ont été utilisés avec succès en combinaison avec des géosynthétiques pour supporter des remblais sur sols mous. Les inclusions par géosynthétique placées sur des pieux sont utilisées pour améliorer le transfert de la charge du sol vers les pieux, réduire le tassement total ou différentiel, et augmenter la stabilité des pentes. Un remblai posé sur des pieux renforcés par géosynthétique construit à Berlin, Allemagne, est choisi pour la modélisation numérique et l'analyse. Les pieux encastrés et chapeaux sont installés, on vient construire ensuite la plateforme de transfert constituée de trois couches de géogrille et matériaux granulaires. La méthode des différences finies incorporées dans le code FLAC (Fast Lagrangian Analysis of Continua) 3D a été utilisée pour la modélisation. Dans l'analyse numérique, les pieux sont modélisés en utilisant des éléments de pieu, et le chapeau est modélisé en le considérant comme élastique. Les éléments de géogrille construits dans le code sont utilisés pour représenter le renforcement par géogrille. Le sol de rembali, le sol mou, le sol raide et les matériaux de plateforme ont été considérés comme des matériaux élastiques linéaires avec plasticité parfaite en vérifiant le critère de rupture de Mohr-Coulomb. Les effets des variations du module mou de sol au-dessous du remblai sur les déplacements verticaux, efforts au-dessus des chapeaux de pile, moments de flexion sur des piles, et la tension dans les renforts ont été étudiées. Les tassements du remblai est calculé et analysé en comparant avec les mesures réelles.

1 INTRODUCTION

Piles or columns, in combination with geosynthetics, have been successfully used to reduce total and differential settlements of embankments over soft soil by transferring most loads from the embankment above the soft soil to piles below (Han and Gabr, 2002). The geosynthetic-reinforced pile-supported embankment system has provided an effective alternative to rapid construction of embankments over soft soil. Due to considerable potential total and differential settlements, a 100-year old double track railway with a length of 2100m in Berlin, Germany was rebuilt in 1994 to 1995 by adopting a geosynthetic-reinforced pile-supported embankment system to support a high-speed (160-200kph) railway (Gartung et al., 1996; Brandl et al., 1997; Zanzinger and Gartung, 2002). The new railway embankment was built on the existing embankment area, which consists predominantly of peat and soft organic silt underlain by medium dense sand encountered at varying depths between 5 and 30 meters. The groundwater table is near the surface. However, because the soil below the old embankment has experienced about 100 years of consolidation, the design parameters for the soil below the embankment and the soil adjacent to the embankment differ greatly. The soft soil below the old embankment base has a natural moisture content of 100 to 350%, while the natural moisture content adjacent to the railway embankment is 300 to 850%. Similar phenomena could be found in terms of the soil moduli and undrain shear strength, which typically range from E_s=0.2 to 0.8 MPa and c_u=2 to 6 kPa outside the embankment and E_s=2 to 6 MPa and c_u=11 to 15 kPa below the existing embankment (determined from triaxial tests). At certain locations, the soil modulus below the existing embankment reaches 8MPa. The friction angles of these soils range from 15^o to 20^o.

Precast piles and caps were installed as shown in Figure 1. The diameter and the length of these piles are 0.118m and 10m to 25m (20m in the section of instrumentation), respectively. They were spaced at a distance of 1.9 m in the x-direction (perpendicular to the traffic direction) and 2.15m in the y-direction (parallel to the traffic direction), respectively. For clarity, the three piles from the centerline of the embankment towards the edge are referred herein to as the center, the middle, and the edge piles, respectively. The required ultimate load capacity of these piles is 1,000 kN. Rectangular precast concrete caps having a dimension of 1.0 m x 1.25m x 0.5m were connected to the piles. Three layers of geogrid, which have a short-term tensile strength of 150 kN/m and a tensile stiffness of 1,100 kN/m, were placed at 5 cm, 25 cm, 50 cm above the pile caps, respectively. The geogrid layers and well-graded gravelly sand form a 0.45m thick load transfer platform. The embankment fill above

the platform is medium to coarse sand, compacted to 97% of Standard Proctor maximum density at which the angle of internal friction is approximately 35°.

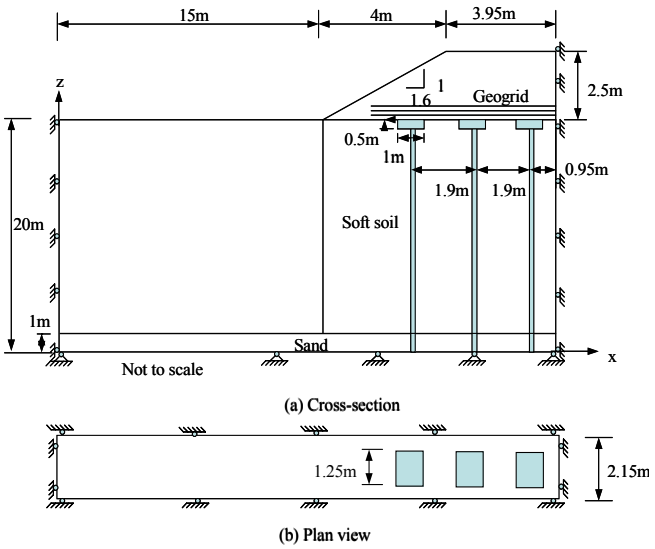

Figure 1. Design Sections and Model for Analysis

2 INSTRUMENTATION AND RESULTS

In order to gain quantitative information on the performance of the geogrid-reinforced pile-supported embankment, the embankment was instrumented with strain gauges, extensometers, acceleration transducers, and conventional surveying. The measurements include settlements and horizontal displacements of the geogrid-reinforced embankment, strains of the geogrid layers between the piles and above the piles, displacements and tilt of the pile caps, and strains of the piles near their tops. Details of these measurements can be found in references by Gartung et al. (1996); Brandl et al. (1997); and Zanzinger and Gartung (2002).

Two key settlement monitoring points (V1.1 and V2.1) were placed at the base of the embankment and located at the midpoints between the pile caps as shown in Figure 2. The measured settlements versus time are plotted in Figure 3. As shown in Figure 3, the settlements increased significantly during the construction of the embankment from 1994 to 1995. In 1996, the rate of the settlement slowed down to approximately 2mm/year. The results also show that the settlement between the center and the middle pile caps is greater than that between the middle and the edge pile caps. The maximum settlements at the end of 2001 reached 60 mm between the center and the middle pile caps and 40 mm between the middle and the edge pile caps, respectively. In addition, the measured settlements above the centers of the pile caps ranged from 7.5 mm to 15mm.

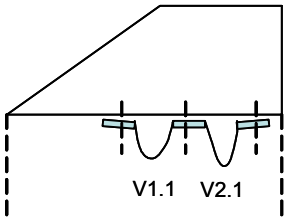

Figure 2. Key measurement points for settlements

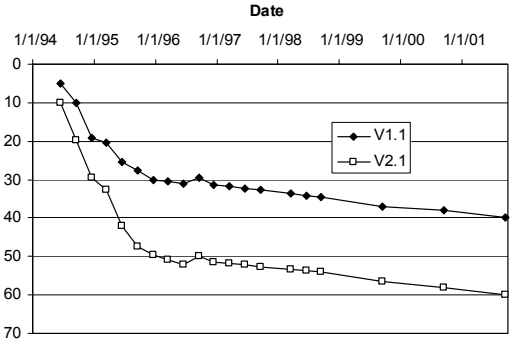

Figure 3. Measured settlement at Point V1.1 and V2.1 (Zanzinger and Gartung, 2002)

A numerical study was conducted by Huang et al. (2005) to investigate the performance of this geosynthetic-reinforced pile supported embankment using the average moduli of the soft soils (i.e., 4MPa underneath the embankment and 0.5MPa outside the embankment). However, the soft soils have a wide range of moduli and their influence on the performance is unknown. This paper will examine the effects of modulus of the soft soil on the performance of the geosynthetic-reinforced pile-supported embankment. The soft soil modulus underneath the embankment used in this study is 2MPa, 4MPa, or 8MPa. To isolate the influence of the soft soil outside the embankment, its modulus is kept constant as 0.5MPa.

3 NUNERICAL ANALYSIS

The finite difference software FLAC (Fast Lagrangian Analysis of Continua) 3D Version 2.1, developed by Itasca Consulting Group, Inc., was adopted for this numerical analysis. The cross-section of the numerical model for this case study is presented in Figure 1.

Due to the symmetry of the problem, half of the section was used in the analysis. The bottom boundary is fixed in all three directions and the four sides are free to move in two directions. The parameters used in the numerical analysis are presented in Table 1.

Table 1. Material Properties used in the Numerical Analysis

Material	Properties
Soft soil (inside)	E=2MPa or 4MPa or 8MPa, ν=0.3, γ=14kN/m^3, c′=12.5kPa, ϕ′=15°
Soft soil (outside)	E=0.5MPa, ν=0.3, γ=14kN/m^3, c′=6.5kPa, ϕ′=15°
Sand	E=40MPa, ν=0.2, γ=18kN/m^3, c′=0kPa, ϕ′=34°
Embankment fill	E=60MPa, ν=0.2, γ=18kN/m^3, c′=0kPa, ϕ′ = 35°
Pile	E=45GPa, ν=0.2, γ=24kN/m^3, K_n=8GN/m/m, K_s=5.1GN/m/m
Pile cap	E = 45GPa, ν = 0.2, γ =24kN/m^3
Geogrid	J=1,100kN/m, c_a=0kPa, δ=32°, k_s=55MN/m/m^2

Note: E = elastic modulus, ν = Poisson's ratio, γ = unit weight, c' = effective cohesion, ϕ′ = effective friction angle, J = tensile stiffness of geotextile, c_a = interface cohesion between geogrid and fill, and δ = interface friction angle between geogrid and fill, K_s = shear stiffness per unit length between pile and soil, K_n = normal stiffness per unit length between pile and soil, k_s = shear stiffness per unit area between geogrid and soil.

In this model, the piles were modeled by using pile elements which were incorporated in FLAC3D. This 3D model contains one row of piles in the x-direction for reducing the computation time. Piles and pile caps were modeled as elastic solid materials. Elastic moduli of piles and pile caps were estimated from in-situ load test data (Brandl et al., 1997). Typical Poisson's ratio was

selected for the piles and the pile caps. Since no detailed information was provided regarding the pile-cap connection, a free rotational and slaved translational connection is assumed. The soft soil (inside or outside the existing embankment area), the dense sand layer underlying the soft soil, and the embankment fill were modeled as elastic-perfectly plastic materials with Mohr-Coulomb failure criterion. The elastic moduli of the sand and the embankment fill were selected based on the suggested values for medium to dense sand (by Budhu, 2000). Geogrid elements (one special type of shell elements), built in the FLAC software, were used to model the three geogrid layers. The geogrid layers were assumed to have isotropic properties with tensile stiffness of 1,100 kN/m, which was determined based on laboratory tensile and creep tests. Adding embankment fill in layers simulates the construction sequence. The side slope was not well defined in all the publications. The appearance of the two benched slopes with steep slope angles (>45^o) would not ensure their stability in the numerical analysis. The benched slopes were simplified to one slope with the same average slope angle in the numerical analysis. In addition, a thin layer (0.2m in thickness) of soil along the slope was assigned with very high strength ($c' = 1{,}000$MPa) to avoid the surficial failure of the slope. A surcharge of 120 kPa was used to simulate the high-speed train loading. This problem was analyzed based on a drained condition. Prior to the analysis, boundary effects of the model were investigated. The current model has minor boundary effects on the results.

Due to the page limit requirements for this paper, only the stress and displacement analyses of the embankment and piles are presented.

4 CALCULATED RESULTS AND COMPARISON

4.1 *Stress analysis*

4.1.1 *Stress distribution above pile caps*

The vertical stresses above pile caps are presented in Figure 4. It is clearly shown that the stresses directly above the pile caps are much higher than those between pile caps. In other words, stress concentration develops above the pile caps. Figure 4 also shows that the vertical stresses above each pile cap are not uniform. The stresses near the edges of pile caps are higher than those in the center of pile caps. This result is in agreement with that found by Han and Gabr (2001). In addition, the stress distribution above the pile cap depends on the location of the pile. The vertical stresses above the edge pile cap are lower than those above the middle and the center piles. This difference is mainly induced by the distribution of the load from the embankment. The soft soil modulus beneath the embankment, was varied from 2MPa to 8MPa in this study, and has only a minor influence on the stress distribution above the pile caps.

4.1.2 *Bending moments on piles*

The distribution of bending moments along the piles is presented in Figure 5. For clarity, the bending moments for the middle pile are not plotted in this figure, however, their magnitudes are close to those for the edge pile. Since free rotation was assumed for the connection between piles and caps, no bending moment develops at the top of the piles. Figure 5 shows that the bending moments along the edge pile (similar to the middle pile) are significantly greater than those along the center pile. This comparison is intuitively correct because the lateral thrust induced by the embankment fill is less near the centerline. The influence of the soft soil modulus beneath the embankment on the bending moments is not significant for the edge pile. For the center pile, however, the increase of the soft soil modulus increases the bending moments of the top one-third of the pile but reduces those of the middle one-third of the pile. The change of the bending moments of the bottom one-third of the pile is not significant.

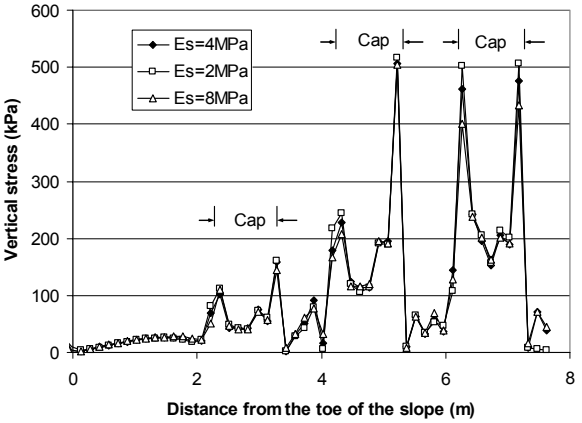

Figure 4. Vertical stresses at the elevation above pile caps in the x-direction

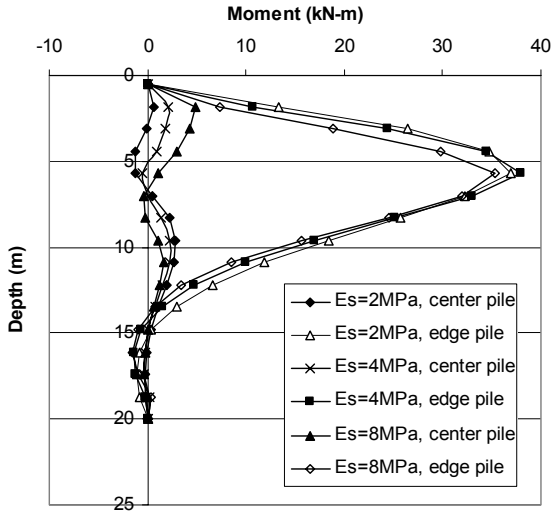

Figure 5. Bending moment distribution along piles in the x-direction

4.1.3 *Tension in reinforcement*

The tension distribution along three geosynthetic reinforcements is presented in Figure 6. For the lower reinforcement layer, the maximum tension develops between the center and the middle pile caps while for the middle and the upper reinforcement layers the maximum tension develops at the edges of pile caps. This behavior can be explained using the "beam" effect as discussed by Huang et al. (2005). From the toe to the centerline of the embankment, the maximum tension in each reinforcement layer develops between the middle and the center piles and not between the center pile and the centerline of the embankment. This implies that the tension in reinforcement is not only induced by the deflection of the reinforcement between pile caps but also induced by the lateral thrust from the embankment fill since the lateral thrust between the middle and center piles is higher than that at the centerline.

The influence of the soft soil modulus beneath the embankment on the maximum tension in the reinforcement is presented in Figure 7. It is clearly shown that the maximum tension in reinforcement decreases with an increase of the soft soil modulus. Figure 7 also shows that the maximum tension in the lower reinforcement is higher than that in the middle and the upper reinforcement. The maximum tension in the middle reinforcement is close to that in the upper reinforcement. However, the calculated tension in reinforcement is higher than the measured ten-

sion. This may possibly be due to the fact that the measurements were reported only reported to March 1996 and the numerical model considered long-term drained conditions.

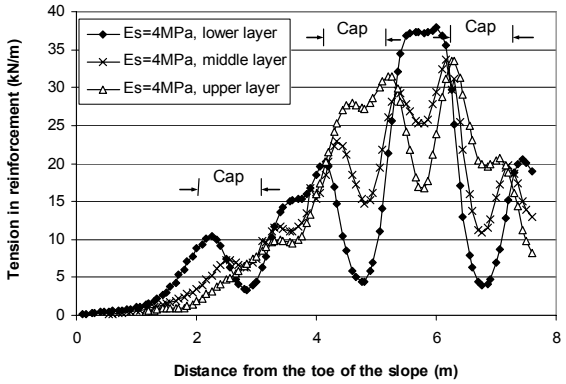

Figure 6. Tension distribution in reinforcement in the x-direction

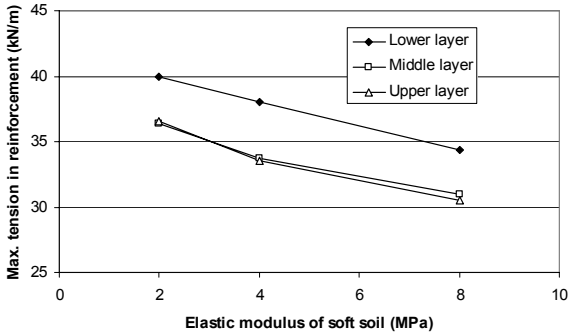

Figure 7. Influence of the soft soil modulus on the maximum tension in reinforcement

4.2 *Displacement analysis*

Figure 8 shows the numerical results of the vertical displacement (settlement) profile at the base of the embankment along the x-axis, which is similar to that shown in Figure 3 based on the field measurements. The figure also shows the tilt of the pile caps and the catenary shape of the deformed geogrid sheet. The rotation of the center and the middle pile caps is the same as that measured in the field. However, the edge pile cap tilts the oposite direction from that measured in the field. This difference may result from the simplification of the side slope and the abrupt difference in soil moduli below and outside the embankment in the numerical analysis.

The settlements at the locations V1.1 and V2.1 and above the centers of the pile caps from the field measurements and the numerical analyses are compared in Table 2. The numerical results based on the soft soil modulus E_s = 2 to 4MPa yield a reasonable agreement with the measured results.

Table 2. Calculated and Measured Settlements (unit: mm)

Method	Modulus, E_s (MPa)	Between pile caps		At the center of pile caps	
		V1.1	V1.2	Min.	Max.
Numerical	2	38.1	62.1	9.5	18.1
	4	34.5	58.5	9.5	17.5
	8	25.7	47.8	8.8	16.0
Measured		40.0	60.0	7.5	15

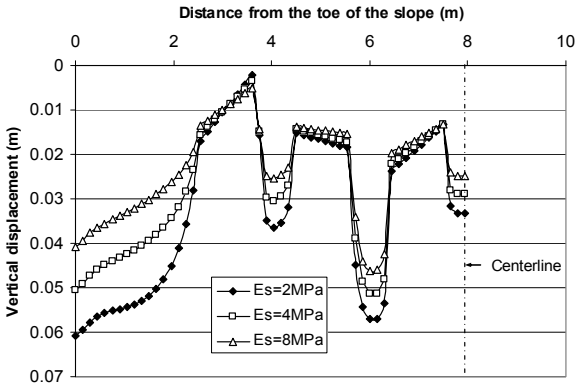

Figure 8. Settlement profile in the x-direction from numerical analysis

5 CONCLUSIONS

The numerical analysis indicates that stress concentration develops above the pile caps and the edge piles are subject to large bending moments. The maximum tension in the lower reinforcement occurs between pile caps while that in the middle and the upper layers occurs near the edges of pile caps. The shape of the deformed geogrid sheet between pile caps is catenary. The tilting of pile caps exists in the cross-section direction to the embankment. The comparisons demonstrate that the 3D numerical method with a simple linear-elastic perfectly plastic model of soils can reasonably well predict the deformations of a geosynthetic-reinforced pile-supported railway embankment.

ACKNOWLEDGEMENTS

This research work was sponsored by the Federal Highway Administration Pooled Fund. This support is greatly appreciated. The authors also would like to thank Mr. Michael Adams and Mr. Christopher Dumas at the Federal Highway Administration for their management and support.

REFERENCES

Alexiew, D. and Gartung, E. (1999) "Geogrid Reinforced Railway Embankment on Piles Performance Monitoring 1994-1998." 1st South American Symposium on Geosynthetics, Brazil, 403-411.

Brandl, H., Gartung, E., Verspohl, J., and Alexiew, D. (1997). "Performance of a geogrid reinforced railway embankment on piles." *Proc. of the Fourteenth Int. Conf. On Soil Mechanics and Foundation Engineering*, Hamburg, 6-12 Sept, Vol. 3, 1731-1736.

Budhu, M. (2000). *Soil Mechanics & Foundations*. John Wiley & Sons Inc, 586p.

Gartung, E., Verspohl, J., Alexiew, D., and Bergmair, F. (1996) "Geogrid reinforced railway embankment on piles-Monitoring." *Geosynthetics: Application, Design and Construction*, De Groot, Den Hoedt & Termaat(eds), Balkema, Rotterdam, 251-258.

Han, J. and Gabr, M.A. (2002). "A numerical study of load transfer mechanisms in geosynthetic reinforced and pile supported embankments over soft soil." Journal of Geotechnical and Geoenvironmental Engineering, ASCE, 128(1), 44-53.

Huang, J., Han, J., and Collin, J.G. (2005). "Geogrid-reinforced pile-supported railway embankments – three dimensional numerical analysis." Submitted to the Annual Transportation Research Board Meeting, Washington, DC.

Itasca Consulting Group Inc. (2002). *FLAC3D Command Reference*, 1st Edition, 358p.

Zanzinger, H. and Gartung, E. (2002) "Performance of a geogrid reinforced railway embankment on piles." *Geosynthetics-7th ICG*-Delmas, Gourc & Girard, Swets & Zeitlinger, Lisse 381-386.